Valery F. GREMENOK[1], Kotte T. Ramakrishna REDDY[2], Mikhail S. TIVANOV[3], Aleksy PATRYN[4]

State Scientific and Production Association «Scientific-Practical Materials Research Centre of the National Academy of Sciences of Belarus» (1), Sri Venkateswara University, Department of Physics, Solar Photovoltaic Lab (2), Belarusian State University (3), Koszalin University of Technology, Department of Electronics and Computer Sciences (4)

doi:10.15199/48.2017.08.23

Effect of annealing on the Structure of thermal evaporated In_2S_3 thin films

***Abstract**. Structural studies on In_2S_3 thin films deposited by vacuum thermal evaporation on glass substrates at a temperature of 240°C, followed by annealing at 330°C and 400°C are presented. It was shown that the films were of amorphous in nature before annealing and after annealing the films became polycrystalline and showed β- In_2S_3 structure. The grain size increased and followed the usual crystal growth process as the annealing temperature increased. The annealing-induced changes of surface roughness were characterized by atomic force microscopy.*

***Streszczenie**. Przedstawiono wyniki badania struktury cienkich warstw In_2S_3 naniesionych metodą termicznego osadzenia na szkło w próżni w temperaturach od 240°C i kolejnym wygrzewaniem w temperaturach 330°C i 400°C. Ustalono że warstwy miały amorficzną naturę przed wygrzewaniem, po wygrzewaniu wykazywały strukturę polikrystaliczną typu β-In_2S_3. Rozmiar ziaren powiększał się na skutek aktywnej nuklearyzacji i to przyczyniało się do zwykłej krystalizacji ze wzrostem temperatury. Zmiany zostały przeanalizowane za pomocą AFM. (**Wpływ obróbki temperaturowej na termicznie naparowane cienkie warstwy In_2S_3**).*

Słowa kluczowe: In_2S_3, cienkie warstwy, XRD widma, Raman widma, AFM obraz powierzchni

Introduction

Thin films of III-VI materials have found applications in many areas of science and technology that include optoelectronics and photovoltaics [1, 2]. Among them, In_2S_3 films are excellent candidates for different applications due to their stability, attractive optical properties and photoconductor behavior [3-6]. Especially In_2S_3 thin films are suitable for application in solar energy photovoltaic conversion [7-9]. It may be perspective to form buffer layers for $Cu(In,Ga)Se_2$ thin film solar cells, which may achieve efficiency up to 16.4% [8]. In_2S_3 is a n-type semiconductor that can exist in several polymorphs and this makes the physical properties of In_2S_3 films significantly dependent on the preparation conditions. The future improvement of solar cells therefore requires the scrupulous characterization of thin film surface and micro-structural properties (including phase composition, grain size, and roughness).

X-ray diffraction (XRD) and Raman spectroscopy are well known as most powerful techniques for structural analysis of thin solid films. Surface roughness and topography, which are used to characterize contact surfaces, were examined via Atomic Force Microscopy (AFM) [10]. In practice, the most commonly used parameters for surface roughness description are average surface roughness R_a and root mean square roughness R_{rms} [11, 12]. However, there are also other roughness parameters that give better surface description like skewness of the roughness profile, R_{sk} and kurtosis of the roughness profile, R_{ku}. The reported data on the influence of annealing temperature on these roughness parameters of thermally evaporated In_2S_3 films is very meager.

Earlier, the effect of the annealing temperature and the thickness of the thermally evaporated In_2S_3 films on their optical properties was studied in [13, 14]. However, there is to date a lack of reported studies regarding influence of annealing temperature on the topography and surface roughness of thermally evaporated In_2S_3 films. Hence, the present study is aimed to investigate the microstructural properties of In_2S_3 films in terms of phase composition and surface topographical parameters.

Method and calculation details

The samples of investigated films were produced by a vacuum thermal evaporation of polycrystalline In_2S_3 powder onto glass substrates in the vacuum chamber (less than $5 \cdot 10^{-4}$ Pa) at 240°C temperature and deposition rate of ~ 0.5 nm/s. The thickness of the films used in this investigation was 1.2 μm. The deposited films were subjected to annealing for 60 min at different temperatures, 330°C and 400°C. More detailed description of the synthesis conditions can be found in the papers [13, 14].

In the present investigation, a Siemens D-5000 X-ray diffractometer was used to investigate the crystal structure, present phases and other structural parameters. It uses CuKα radiation (λ = 0.15405 nm) with a nickel filter and the data was recorded over the scattering angle range, 10 – 60 degree. Raman spectra were obtained at a room temperature using a DILOR XY 800 spectrometer. For the excitation of Raman radiation, an Ar-laser with a wavelength of 514.5 nm was used. JEOL JSPM-4210 atomic force microscope was used to study the surface topographical parameters in the noncontact mode.

Results and discussion

Fig. 1 shows XRD spectra of In_2S_3 thin films deposited on glass substrates and annealed at 330°C and 400ºC. It is seen that the films have an amorphous structure after the deposition. The absence of any of In_2S_3 peaks in the as-deposited films is due to the low thermal energy, which is insufficient for significant crystallization [15, 16]. X-ray diffraction spectrum of the In_2S_3 film annealed at 330°C showed low-intensity peaks related to the (214) and (324) crystalline planes of the tetragonal In_2S_3 phase [17]. X-ray diffraction spectrum of the In_2S_3 annealed at 400°C showed the appearance of high-intensity peak near 2θ = 33 deg. corresponding to (220) crystalline plane of tetragonal phase [18]. Additionally, the XRD spectra of the films annealed at 400°C showed diffraction peaks that correspond to the (008), (115), (204), (311), (215) and (422) planes of the cubic In_2S_3 [16]. Previously, co-existence of the cubic and tetragonal phases in In_2S_3 layers grown by the chemical bath deposition was reported in [19]. Besides, a phase change in the evaporated In_2S_3 films with the change of substrate temperature was also reported in [20].

The fact that the full width at half maximum (FWHM) decreased with the raise of annealing temperature is an indicator of improved crystalline quality of thin film. As seen from the Fig. 1, there was an intensity increase for XRD peaks with increasing annealing temperature. This may be due to thermal energy increase enough for recrystallization

and the grain growth. The crystallite sizes were calculated by the Scherrer formula from the peak FWHM [21]

$$D = \frac{0.94\lambda}{\beta \cos\theta},$$

where D is grain size and β is FWHM.

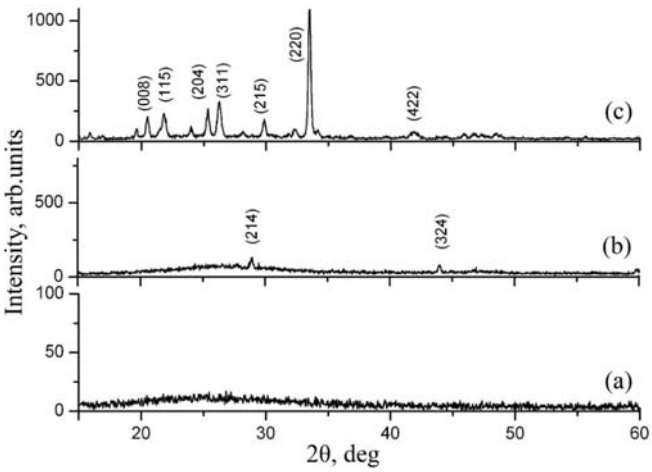

Fig.1. Typical XRD spectra of In_2S_3 thin films: before annealing (a), after annealing at 330°C (b) and at 400ºC (c)

With annealing temperature increasing, the grain size increased from 50 to 75 nm. The smaller grain size for the films annealed at 330°C can be due low mobility and diffusion of the deposited molecules because of lower thermal energy.

Fig. 2 shows Raman spectra of In_2S_3 thin films deposited on glass substrates and annealed at 330°C and 400ºC. After deposition and after annealing at 330°C, the Raman peaks at 164 and 281 cm^{-1} as well as low-intensity peaks at 95 and 131 cm^{-1} indicated the presence of β-In_2S_3 defect spinel, tetragonal, structure [22-23]. Raman peaks at 126, 244 and 260 cm^{-1} corresponding to α- In_2S_3 cubic structure rise after annealing of In_2S_3 films at 400°C [24, 25]. This result demonstrates that the annealing leads to transformation from β- In_2S_3 to α- In_2S_3 phase at temperatures about 400°C.

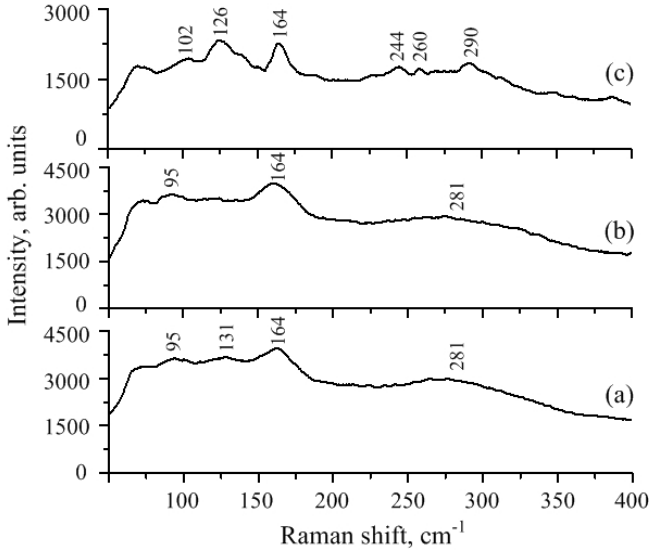

Fig.2. Typical Raman spectra of In_2S_3 thin films: before annealing (a), after annealing at 330°C (b) and at 400ºC (c)

Fig. 3 shows typical 2D and 3D AFM images of In_2S_3 thin films before and after annealing at 330°C and at 400°C. The In_2S_3 thin films are continuous and homogeneous. It is observed from the images that the average height of the roughness profile increases with annealing temperature. The as-deposited films have a granular surface morphology. However, in case of the films annealed at different temperatures, the surface had completely different morphology.

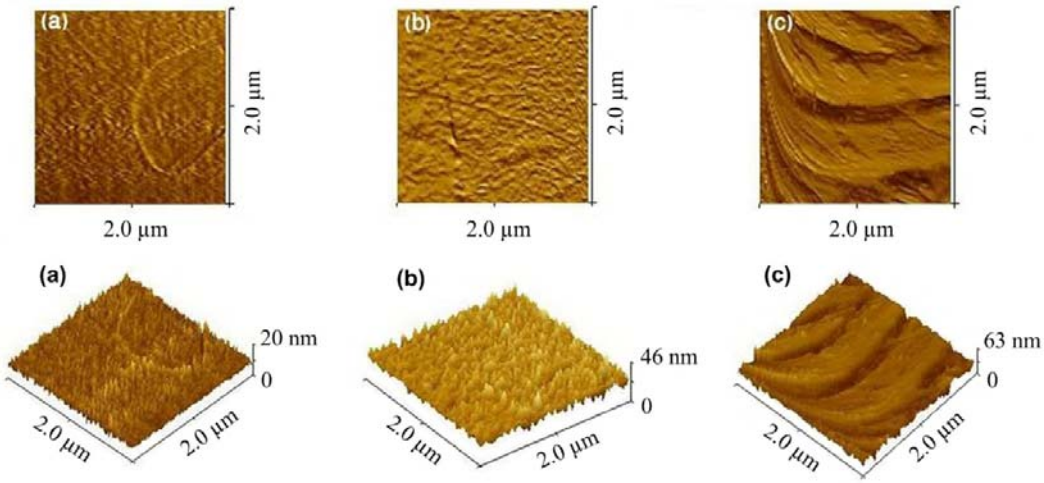

Fig.3. Typical 2D and 3D AFM images of In_2S_3 thin films: before annealing (a), after annealing at 330°C (b) and at 400ºC (c)

Surface roughness analysis of In_2S_3 thin films is presented in Table. The results of the statistical calculation revealed that the height distribution has changed after annealing of the samples. It can be seen that the surface roughness increases with the increase of annealing temperature. Before annealing, the average roughness of thin films was of ~ 1.3 nm. But when the samples were annealed at 400°C, the average roughness increased to ~ 4.0 nm.

Table: Average values obtained from AFM measurements and defined roughness of In_2S_3 thin films

Parameter	Without annealing	Annealed at	
		330°C	400°C
Arithmetic average height, nm	9.40	24.42	31.17
Average roughness R_a, nm	1.30	3.74	3.97
Root mean square roughness R_{rms}, nm	1.68	4.76	5.06
Skewness R_{sk}, nm	0.35	-0.46	-0.42
Kurtosis R_{ku}, nm	0.91	0.65	0.94

The increase of R_a and R_{rms} as the annealing temperature increased corresponds to the improving of In_2S_3 films crystalline quality [26-28]. In Table, change of skewness sign from positive to negative indicates that the formation of protruding grains occurred during the annealing. The kurtosis is a yardstick for the sharpness of a surface, and expresses the sharpness of the height distribution; the height distribution is not sharp at $R_{ku} < 3$ [26]. The results of skewness and kurtosis analysis (Table) showed that the surface of In_2S_3 film becomes generally rough during the annealing, with protruding grains being dominant.

Conclusions

Correlation between the structural properties and the annealing temperature of In_2S_3 thin films was reported. The Raman peaks of In_2S_3 thin films indicating the presence of β- In_2S_3 in the as-deposited samples and after annealing at 330°C. After annealing at 400°C, new peaks related to α- In_2S_3 were observed. Phase transitions after annealing at 400°C resulting in co-existence of both cubic and tetragonal phases in In_2S_3 layers was also detected by XRD analysis. It was found that the increase of annealing temperature leads to greater crystallite sizes, as well as the increased roughness of the films. The values of surface roughness and grain size can be controlled by adjusting the annealing temperature.

These results provide a more comprehensive understanding of the annealing temperature influence on In_2S_3 films structural and morphological features and could help in controlling the topographical parameters according to the surface morphology requirements suitable for photovoltaic applications.

The work was performed with the financial support from the Belarusian Republican Foundation for Fundamental Research (Grant No. T15IND-001), from the Department of Science and Technology (DST), New Delhi (Grant No. DST/INR-BLR/P-29/2014) via the India-Belarus Joint Research Collaboration programme, and from Belarusian State Programme for Research «Physical material science, new materials and technologies».

Authors: *Valery F. Gremenok, State Scientific and Production Association «Scientific-Practical Materials Research Centre of the National Academy of Sciences of Belarus», 19 P. Brovki str., Minsk, 220072 Belarus; Kotte T. Ramakrishna Reddy, Sri Venkateswara University, Department of Physics, Solar Photovoltaic Lab, Tirupati, 517502 India, Mikhail S. Tivanov, Belarusian State University, 4 Nezavisimosti av., Minsk, 220030 Belarus, Aleksy Patryn, Koszalin University of Technology, Department of Electronics and Computer Sciences, 2 Sniadeckich str, Koszalin, 75-453 Poland, E-mail: patryn@ie.tu.koszalin.pl.*

REFERENCES

[1] Seyam M.A., *Vacuum*, 63 (2001), 441-447
[2] Hara K., Sayama K., Arakawa H., *Sol. Energy Mater. Sol. Cells*, 62 (2001), 441-449
[3] Shay J.L., Tell B., *Surf. Sci.*, 37, 748-752 (1973)
[4] George J., Joseph K.S., Prodeep B., *Phys. Status. Solidi. Appl. Res.*, 106 (1988), 123-127
[5] Barreau N., Bernède J.C., Marsillac S., *Thin Solid Films*, 431 (2003), 326-331
[6] Bube R.H., McCarroll W.H., *J. Phys. Chem. Solids*, 10 (1959), 333-340
[7] Naghavi N., Spiering S., Powalla M., Cavana B. and Lincot D., *Prog. Photovolt. Res. Appl.*, 11 (2003), 437-443
[8] Strohm A., Eisenmann L., Gebhardt R.K., Harding A., Schlotzer T., Abou-Ras D., Schock H.W., *Thin Solid Films*, 480-481, 162-167 (2005)
[9] Nehra S.P., Chander S., Anshu Sharma, Dhaka M.S., *Mater. Sci. Semicond. Process.*, 40 (2015), 25-29
[10] Nagabhushana K.R., *Nucl. Instr. Meth. Phys. Res. B*, 266 (2008), 1040-1042
[11] Woka M.K., Ottaviano L., Szuber J., *Thin Solid Films*, 515 (2007), 8328-8332
[12] Lita E., Sanchez J.E., *J. Appl. Phys.,* 85 (1999), 876-881
[13] Izadneshan H., Gremenok V.F., *J. Appl. Spectros.*, 81 (2014), 293-296
[14] Izadneshan H., Gremenok V.F., *J. Appl. Spectros.*, 81 (2014), 765-770
[15] Bhatti M.T., Rana A.M., Khan A.F., *Mater. Chem. Phys.*, 84 (2004), 126-130
[16] Xiong Y., Xie Y., Du G., Tian X., Qian Y., *J. Solid. State. Chem.*, 166 (2002), 33-40
[17] Powder Diffraction File, Joint Committee on Powder Diffraction Standards, ASTM, Philadelphia, PA, 1967, Card 250390
[18] Powder Diffraction File, Joint Committee on Powder Diffraction Standards, ASTM, Philadelphia, PA, 1967, Card 050731
[19] Sandoval M.G., Sotelo-Lerma M., Valenzuela-Jauregui J.J., Flores-Acosta M., Ramirez-Bon R., *Thin Solid Films*, 472 (2005), 5-10
[20] Revathi N., Prathap P., Subbaiah Y.P., Reddy K.T., *J. Phys. D: Appl. Phys.*, 41 (2008), 155404-155408
[21] Cullity D., Elements of X-ray Diffraction, Addison-Wesley Publishing Company Inc., (1956), 262-269
[22] Ursaki V.V., Manjón F.J., Tiginyanu I.M., Tezlevan V.E., *J. Phys.: Condens. Matter*, 14 (2002), 6801-6813
[23] Revathi N., Prathap P., Reddy K.T., *Solid State Sci.*, 11 (2009), 1288-1296
[24] Kambas K., Spyridelis J., Balkanski M., *Phys. Status Solidi*, 105 (1981), 291-296
[25] Tao H., Zang H., Dong G., Zeng J., Zhao X., *Optoelectron. Adv. Mater.*, 2 (2008), 356-359
[26] Raposo M., Ferreira Q., Ribeiro P.A., Modern Research and Educational Topics in Microscopy, FORMATEX, (2007), 758-769
[27] Gadelmawlaa E.S., Kourab M.M., Maksoudc T.M.A., Elewaa I.M., Solimand H.H., *J. Mater. Process. Tech.*, 123 (2002), 133-140
[28] Wysocka K., Ulatowska A., Bauer J., Holowacz I., Savu B., Stanciu G., *Optica Applicata*, 38 (2008), 130-135